Controlling Association of Vesicle Embedded Peptides by Alteration of the Physical State of the Lipid Matrix†

Natascha Naarmann,‡ Başar Bilgiçer,§ Krishna Kumar,*,§,|| and Claudia Steinem*,‡

Institut für Analytische Chemie, Chemo- und Biosensorik, Universität Regensburg, 93040 Regensburg, Germany, Department of Chemistry, Tufts University, Medford, Massachusetts 02155-5813, and Cancer Center, Tufts-New England Medical Center, Boston, Massachusetts 02110

Received January 17, 2005; Revised Manuscript Received February 1, 2005

ABSTRACT: We report here the reversible association of a designed peptide embedded in a lipid membrane through a stimulus-sensitive trigger that changes the physical state of the bilayer matrix. A peptide designed with the classical 4-3 heptad repeat of coiled coils, equipped with leucine residues at all canonical interface positions, **TH1**, was rendered membrane soluble by replacement of all exterior residues with randomly selected hydrophobic amino acids. Insertion of **TH1** into large unilamellar phosphatidylcholine vesicles was followed by monitoring tryptophan fluorescence. Peptide insertion was observed when the lipids were in the liquid-crystalline state [1-palmitoyl-2-oleoyl-*sn*-glycero-3-phosphocholine (POPC)] but not when they were in the crystalline phase [1,2-dipalmitoyl-*sn*-glycero-3-phosphocholine (DPPC)]. Formation of a trimeric α-helical bundle in lipid bilayers was followed by fluorescence resonance energy transfer. Global fit analysis revealed a monomer−trimer equilibrium with a dissociation constant of around 10^{-6} MF^2. A lipid mixture composed of DPPC and POPC exhibiting a phase transition at 34 °C between a crystalline/liquid-crystalline coexistence region and a completely miscible liquid-crystalline phase was used to control the formation of the trimeric peptide bundle. **TH1** is phase excluded in crystalline DPPC domains below 34 °C, leading to a larger number of trimers. However, when the DPPC domains are dispersed at temperatures above 34 °C, the number of trimers is reduced.

Approximately one-third of all open reading frames in sequenced genomes encode transmembrane proteins (*1*). Two motifs appear to dominate the structural arrangements of such proteins, α-helical bundles and *β*-barrels (*2*). The former structural class has been observed in many of the well-characterized integral proteins, including glycophorin A (*3*−*5*), M13 major coat protein (*6*), phospholamban (*7*, *8*), T-cell receptor (*9*), and MHC-II[1] complex (*10*). Engelman and co-workers have proposed that the folding and assembly of membrane proteins may follow two energetically independent steps involving the insertion of, followed by intermolecular interaction between, preformed helices within the cellular membrane (*11*, *12*). This model provides a useful and convenient starting point for advancing our understanding of helix−helix interactions within membranes (*13*). In this report, we demonstrate the modulation and reversible association in vesicles of a transmembrane α-helical bundle by altering the physical state of the lipid matrix.

Analysis of the structural features of packing and relative alignment of interacting helices within membranes has revealed that it is reminiscent of the "knobs-into-holes" packing observed in soluble coiled coils (*14*). Indeed, the long axes of interacting helices in coiled coils prefer a left-handed crossing angle of ∼ 20°, closely matching the average value found in helical membrane proteins. Coiled coils are ubiquitous protein motifs that engage in a large variety of functions by forming superhelical oligomers of α-helices (*15*−*17*). They are frequently part of oligomerization domains and are characterized by a 4-3 hydrophobic heptad repeat resulting in an extended surface amphiphilic in nature that templates oligomer formation (*18*−*20*). Further evidence of the structural correspondence was made apparent when an integral membrane protein phospholamban was rendered soluble by replacing the membrane-exposed hydrophobic residues with polar and charged residues (*21*, *22*).

Zhou et al. (*23*) have described a model transmembrane helical system based on the coiled coil region of bZIP transcriptional activator GCN4 and investigated its association properties in SDS detergent micelles and in vivo by using a chimeric construct with staphylococcal nuclease (TOXCAT). Interhelical association was promoted by a central asparagine, independent of the rest of the sequence composed of valine and/or leucine residues. DeGrado and

† This work was supported in part by National Institutes of Health Grants GM65500 and 1S10RR017948 and by National Science Foundation Grants CHE-0236846 and CHE-0320783. Additional support to C.S. was provided by the Fonds der Chemischen Industrie. K.K. is a DuPont Young Professor.

* To whom correspondence should be addressed. C.S.: phone, +49 (941) 943-4548; fax, +49 (941) 943-4491; e-mail, claudia.steinem@chemie.uni-regensburg.de. K.K.: phone, (617) 627-5651; fax, (617) 627-3443; e-mail, krishna.kumar@tufts.edu.

‡ Universität Regensburg.

§ Tufts University.

|| Tufts-New England Medical Center.

[1] Abbreviations: DMSO, dimethyl sulfoxide; DPC, dodecylphosphocholine; DPPC, 1,2-dipalmitoyl-*sn*-glycero-3-phosphocholine; FRET, fluorescence resonance energy transfer; LUV, large unilamellar vesicle; MHC, multihistocompatibility complex; POPC, 1-palmitoyl-2-oleoyl-*sn*-glycero-3-phosphocholine; NBD, nitrobenz-2-oxa-1,3-diazole; SDS, sodium dodecyl sulfate; TAMRA, 5(6)-carboxytetramethylrhodamine.

10.1021/bi050096f CCC: $30.25 © 2005 American Chemical Society
Published on Web 03/10/2005

co-workers (*24*) also designed transmembrane peptide helices starting from the GCN4 coiled coil region, which was converted into a membrane-soluble peptide by changing the exterior polar side chains of the water-soluble peptide to apolar side chains, while the buried side chains were kept invariant. Analytical ultracentrifugation, SDS electrophoresis, and fluorescence resonance energy transfer provided evidence for the formation of aggregates in a variety of micellar systems, including C12E8, DPC, SDS, and C14-betaine (*25*). The critical amino acid responsible for association again appeared to be a central asparagine. If asparagine was replaced with valine, the corresponding peptide failed to associate in micelles (*24*).

Here we report that the association of peptide system **TH1**, based on the heptad repeat of coiled coils, can be modulated by the organization of the lipid membrane. For the past three decades, the biological membrane has been viewed as a homogeneous fluid lipid matrix with embedded proteins, according to the fluid mosaic model. However, this picture has been reinvented in recent years by the idea that the membrane is a structured system with a nonuniform distribution of proteins and lipids. A new term to describe small domains in membranes has been coined ("lipid rafts") (*26*), and it is thought that within these supramolecular transient structures, certain proteins are located preferentially or even solely while others are excluded. Thus, the organization of the lipid matrix might be used to control the localization of peptides and proteins and even dictate the overall organization and folding of a certain peptide structure. Our results suggest that stimulus-induced changes in the organization of lipid vesicles can be used to control the oligomeric state of transmembrane peptides, and this may be a mechanism prevalent in nature.

EXPERIMENTAL PROCEDURES

Materials. **TH1**, 7-nitrobenz-2-oxa-1,3-diazole (NBD)-**TH1**, and 5(6)-carboxytetramethylrhodamine [5(6)-TAMRA]-**TH1** were synthesized as described elsewhere (*13*). 1-Palmitoyl-2-oleoyl-*sn*-phosphocholine (POPC) and 1,2-dipalmitoyl-*sn*-glycero-3-phosphocholine (DPPC) were purchased from Avanti Polar Lipids (Alabaster, AL). Patman [6-hexadecanoyl-2-({[2-(trimethylammonium)ethyl]methyl}amino)-naphthalene chloride] was provided by M. Hof (J. Heyrovský Institute of Physical Chemistry, Academy of Sciences of the Czech Republic, Prague, Czech Republic).

Vesicle Preparation. Large unilamellar vesicles (LUVs) composed of 1-palmitoyl-2-oleoyl-*sn*-glycero-3-phosphocholine (POPC), 1,2-dipalmitoyl-*sn*-glycero-3-phosphocholine (DPPC), and a mixture of POPC and DPPC in a molar ratio of 4:6 with the corresponding amount of peptide were prepared according to the extrusion method. First, lipids dissolved in chloroform and peptides dissolved in ethanol were added to a glass tube, and the solvent was evaporated under a stream of nitrogen followed by several hours under vacuum resulting in a lipid−peptide film. For the determination of the phase transition of POPC/DPPC (4:6) vesicles, Patman dissolved in ethanol was added to the lipids before evaporation, resulting in a lipid-to-Patman ratio of 100:1. The temperature was adjusted to a value above the main phase transition temperature of the lipid or lipid mixture. For POPC, all processes were performed at room temperature, while for the POPC/DPPC mixture, the preparation was carried out at 50 °C, well above the main phase transition temperature of pure DPPC (T_m = 41.5 °C). Multilamellar vesicles were obtained by swelling the lipid−peptide film in water for 30 min with periodic vortexing for 30 s. The resulting multilamellar vesicles were then sized by extrusion through stacked polycarbonate membranes with nominal pore diameters of 100 nm using a miniextruder (LiposoFast, Avestin) to obtain large unilamellar vesicles.

Determination of Peptide Concentrations. Concentrations of the unlabeled peptide were determined by UV spectroscopy using the absorbance of the single tryptophan residue (ϵ_{280} = 5690 M^{-1} cm^{-1}), while those of the labeled peptides were determined by the absorbance of NBD (ϵ_{460} = 23 000 M^{-1} cm^{-1}) and TAMRA (ϵ_{550} = 92 000 M^{-1} cm^{-1}).

Insertion of Peptides in Lipid Bilayers. Insertion of **TH1** into lipid bilayers, as well as the reversibility of insertion, was investigated by monitoring tryptophan fluorescence. Fluorescence emission spectra were recorded on a Cary Eclipse fluorescence spectrometer (Varian, Darmstadt, Germany). The spectra, obtained by excitation at 280 nm, were recorded in the wavelength range of 290−450 nm, while the solution was continuously stirred. Fluorescence spectra were corrected for vesicle scattering and dilution of the peptide solution if necessary. Excitation and emission bandwidths were set at 5 nm. The spectra were collected at room temperature.

Peptide insertion in lipid vesicles was accomplished in two different ways. In the first approach, peptides were dissolved in a H_2O/DMSO mixture (8:2) and diluted in 10 mM Tris and 100 mM NaCl (pH 7.5) at a concentration of 0.02 mg/mL, and preformed lipid vesicles at a concentration of 3.0 mg/mL were added stepwise, leading to a lipid-to-peptide ratio in the range of 0−1200:1. During vesicle addition, the suspension was incubated for approximately 20 min until the tryptophan fluorescence intensity remained constant, indicating that equilibrium had been reached. In a second approach, mixed lipid−peptide films were prepared as described above. The peptide concentration was kept constant at 0.02 mg/mL. The lipid-to-peptide ratio was increased by varying the lipid concentration in the range of 0−1100:1.

To investigate whether the peptides, once inserted into a lipid bilayer, stay in one vesicle or can switch between different vesicles, the procedure of Wimley et al. (*27*) was followed. Four different vesicle populations were prepared: (1) pure POPC vesicles, (2) POPC vesicles doped with the quencher 5-DOXYL-stearic acid (15 mol %), (3) POPC vesicles with inserted peptide **TH1**, and (4) POPC vesicles doped with the quencher 5-DOXYL-stearic acid (15 mol %) and **TH1**. The peptides were inserted by the two different methods as described above. In the case of addition of the peptide after the vesicle formation process, suspensions 3 and 4 were incubated for 1 h after peptide addition to ensure complete peptide insertion and equilibrium. In parallel, two different mixtures were prepared from the four different vesicle suspensions. One mixture contained suspensions 1 and 4, while the other one contained suspensions 2 and 3. For each insertion procedure, mixtures of suspensions 1 and 4 and suspensions 2 and 3 were incubated for 30 min before the first fluorescence spectrum was recorded. Full and reversible exchange of the peptides was assumed when the observed tryptophan fluorescence intensity was intermediate

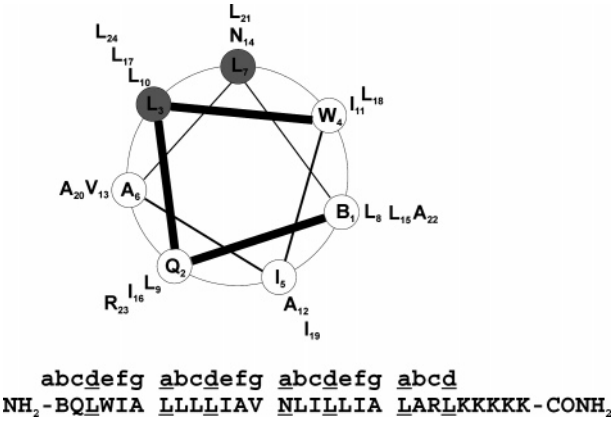

FIGURE 1: **TH1** is shown in a helical wheel representation assuming a 4-3 heptad repeat and a pitch of 3.5 residues per turn. Residue B denotes β-alanine (CAS Registry No. 107-95-9).

to the original intensity of suspensions 3 and 4 and identical in the two different mixtures.

Assessment of Peptide Association. Association of **TH1** in lipid bilayers was monitored by fluorescence resonance energy transfer (FRET) at various lipid-to-peptide ratios. NBD-labeled peptides served as fluorescence donors, while TAMRA-labeled peptides served as acceptors. Each spectrum was corrected by subtracting the spectrum of a corresponding vesicle suspension lacking the fluorescently labeled peptides. Fluorescence emission was monitored between 500 and 700 nm with excitation at 485 nm, while the solution was continuously stirred at room temperature. The total peptide concentration was kept constant at 5.5 μM using an unlabeled peptide. Different lipid-to-peptide ratios were investigated by changing the POPC concentration: 900:1 (1.65 mM POPC), 600:1 (3.30 mM POPC), and 300:1 (4.95 mM POPC). The samples were prepared in water and diluted with 10 mM Tris and 100 mM NaCl (pH 7.5).

The temperature dependence of the fluorescence resonance energy transfer was followed by monitoring the donor fluorescence intensity at 430 nm between 10 and 50 °C at a scan rate of 30 °C/h. LUVs composed of DPPC and POPC in a molar ratio of 6:4 were used. A total lipid concentration of 3.30 mM and peptide concentrations of 2.75 μM NBD-**TH1**, 2.48 μM 5(6)-TAMRA-**TH1**, and 0.27 μM **TH1** [$c_{NBD}/c_{5(6)-TAMRA} = 0.9$] were adjusted, which correspond to a lipid-to-peptide ratio of 600:1. As a control, DPPC/POPC LUVs were prepared in which the acceptor peptide, 5(6)-TAMRA-**TH1**, was substituted with the unlabeled peptide.

Determination of the Phase Transition Temperature. The phase transition temperature T_m of the DPPC/POPC mixture (molar ratio of 6:4) was determined by monitoring the fluorescence maximum λ_{max} of the fluorophore Patman in a temperature range of 10−50 °C at a scan rate of 30 °C/h. Fluorescence emission spectra between 400 and 600 nm with an excitation wavelength of 360 nm were recorded. A lipid concentration of 1.34 mM with a lipid-to-Patman ratio of 100:1 was used.

RESULTS

Insertion of the Peptide into Lipid Vesicles. Integration of peptide **TH1** (Figure 1) into phospholipid vesicles was followed by monitoring the fluorescence emission of tryptophan. After the transition from a high-dielectric (water) to a low-dielectric medium (lipid phase), a blue shift in tryptophan fluorescence is observed concomitant with an increase in intensity (*28*). Two different vesicle populations were employed, 1,2-dipalmitoyl-*sn*-glycero-3-phosphocholine (DPPC) which is in the crystalline state and 1-palmitoyl-2-oleoyl-*sn*-glycero-3-phosphocholine (POPC) which is in the liquid-crystalline state at room temperature. In a first set of experiments, vesicles were added stepwise to an aqueous solution of the peptide, resulting in different lipid-to-peptide ratios, and the tryptophan fluorescence was monitored. Upon addition of DPPC vesicles to the peptide solution, the fluorescence spectra remained unchanged (data not shown), indicating that **TH1** does not insert into DPPC bilayers at room temperature. However, stepwise addition of POPC vesicles to an aqueous solution of the peptide at room temperature after a 20 min equilibration led to a substantial increase in tryptophan fluorescence intensity (~30%, Figure 2A) and a 21 nm blue shift in λ_{max} (Figure 2B). This observation can be attributed to the transfer of the tryptophan residue from the aqueous phase to the more hydrophobic lipid phase. The results clearly demonstrate that peptide **TH1** inserts into lipids only when they are in the liquid-crystalline state.

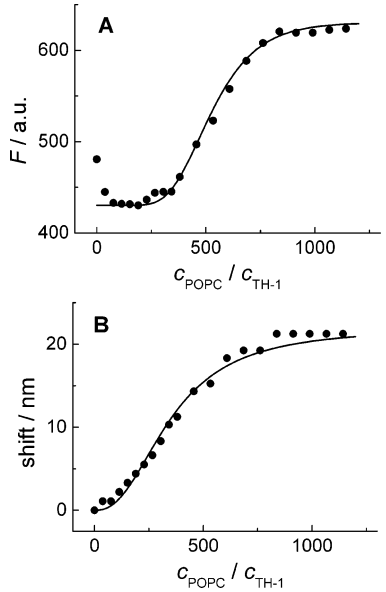

FIGURE 2: Change in tryptophan fluorescence as a function of lipid-to-peptide ratio. A solution containing 3.9 mM POPC LUVs was added stepwise (10 μL) to an aqueous solution (8:2 H_2O/DMSO) of 6 μM **TH1**, and (A) the increase in tryptophan fluorescence intensity or (B) the decrease in λ_{max} was monitored. Prior to vesicle addition, the λ_{max} of the peptide solution was determined to be 358 nm.

In a second set of experiments, **TH1** was added directly to the lipid film and large unilamellar vesicles were formed in the presence of the peptide. Tryptophan emission spectra of POPC vesicles harboring **TH1** (lipid-to-peptide-ratio of 600:1) displayed a λ_{max} of 337 nm as opposed to a λ_{max} of 358 nm for the peptide in the aqueous phase. The observed magnitude of the blue shift can be reproduced if the peptide is added prior to vesicle preparation and supports the location of tryptophan in a low-dielectric environment, namely, well inserted into the vesicles.

The question of whether the peptides, once inserted into a lipid bilayer, stay in one vesicle or move between different vesicles arose, in addition to how the insertion procedure of

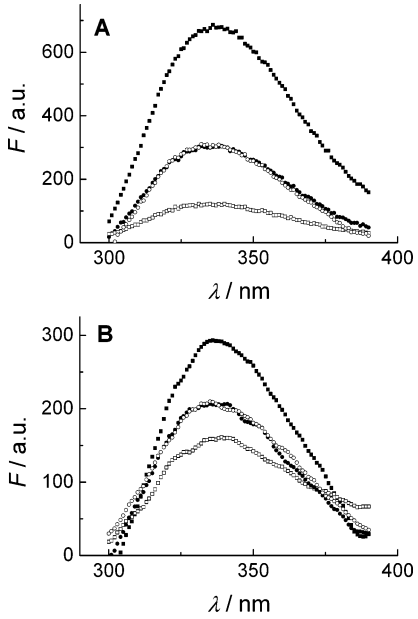

FIGURE 3: (A) Determination of reversibility of peptide insertion. **TH1** insertion was accomplished by adding the peptide to preformed POPC vesicles. Fluorescence emission spectra of suspension 3 (■) and suspension 4 (●) and mixtures of suspensions 1 and 4 (○) and suspensions 2 and 3 (□) are shown. Suspension 1 was pure POPC vesicles, suspension 2 POPC vesicles doped with the quencher 5-DOXYL-stearic acid, suspension 3 POPC vesicles with inserted peptide **TH1**, where no quenching occurs, and suspension 4 POPC vesicles doped with 5-DOXYL-stearic acid and **TH1** (this suspension experiences maximal quenching before mixing). The measurements were performed at a lipid-to-peptide ratio of 575:1 and a peptide concentration of 2.2 μM. (B) Determination of the reversibility of **TH1** insertion in mixed lipid−peptide films after vesicle formation. The fluorescence spectra of suspensions 3 (■) and 4 (●) and mixtures of suspensions 1 and 4 (○) and suspensions 2 and 3 (□) are shown. The measurements were performed at a lipid-to-peptide ratio of 600:1 and a peptide concentration of 2.2 μM.

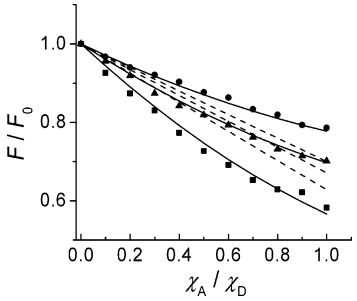

FIGURE 4: Determination of the association state of **TH1** in POPC LUVs. The ratio of fluorescence intensity in the presence (*F*) and absence (F_0) of acceptor as a function of the molar ratio of TAMRA-labeled peptide (acceptor) to NBD-labeled peptide (donor) was monitored, while keeping the total peptide concentration constant at 5.5 μM using the unlabeled peptide. Different lipid-to-peptide ratios were investigated by changing the POPC concentration: (●) 1:900 (1.65 mM POPC), (▲) 1:600 (3.30 mM POPC), and (■) 1:300 (4.95 mM POPC). The solid lines are the results of a fitting procedure using a monomer−trimer equilibrium with a dissociation constant K_D of 4.35×10^{-6} MF^2. The dotted lines are fits to a monomer−dimer equilibrium with a dissociation constant K_D of 6×10^{-4} MF. For the fitting routine, f_Q/f_D was set to zero and X_D was fixed at 0.5.

the peptide influences this process. To address this question, we prepared four different vesicle populations: (1) pure POPC vesicles, (2) POPC vesicles doped with the quencher 5-DOXYL-stearic acid, (3) POPC vesicles with inserted peptide **TH1**, and (4) POPC vesicles doped with the quencher 5-DOXYL-stearic acid and **TH1**. For peptide insertion, unilamellar vesicles were prepared and subsequently **TH1** was added. Suspensions 3 and 4 were then incubated for 1 h to ensure equilibration. Afterward, two different mixtures were prepared from the four different vesicle suspensions in parallel. One mixture contained suspensions 1 and 4, while the other one contained suspensions 2 and 3. For each insertion procedure, mixtures of suspensions 1 and 4 and suspensions 2 and 3 were incubated for 30 min before the first fluorescence spectrum was recorded. Full and reversible exchange of the peptides was assumed when the observed tryptophan fluorescence intensity was intermediate to that of the original intensity of suspensions 3 and 4, and identical in the two different mixtures.

After 24 h, partition equilibrium was reached as concluded from continuously recorded fluorescence spectra demonstrating a constant tryptophan intensity. The final fluorescence spectra are shown in Figure 3A. The intensities of the mixed vesicle population (suspensions 2 and 3 and suspensions 1 and 4, respectively) are intermediate compared to the initial intensities observed for pure POPC vesicles with **TH1** (suspension 3) and POPC vesicles with **TH1** doped with 5-DOXYL-stearic acid (suspension 4). The result clearly shows that the peptides exchange between the different vesicle populations, i.e., the insertion process is fully reversible. The same result was observed if **TH1** was inserted in the lipid film prior to vesicle preparation (Figure 3B). The only difference was that if the peptide was directly added to the lipid film prior to vesicle formation, partition equilibrium was reached faster than when the peptide was added after vesicle formation. For the following experiments, peptide insertion was always accomplished by adding the peptide to the lipid film prior to vesicle formation to ensure complete peptide insertion into the lipid bilayer immediately after the vesicle formation process.

Association of TH1 in Lipid Vesicles. The association state of **TH1** in lipid vesicles was investigated by fluorescence resonance energy transfer (FRET), using NBD-labeled peptides as donors and TAMRA-labeled peptides as acceptors. By measuring the decrease in fluorescence emission intensity of NBD as a function of the acceptor concentration while keeping the total lipid-to-peptide ratio constant by the addition of the unlabeled peptide, one can determine the average degree of association at each lipid-to-peptide ratio (*28*−*32*). Figure 4 shows the ratio of fluorescence intensity *F* in the presence of TAMRA-labeled peptides and F_0, the fluorescence intensity in its absence for different lipid-to-peptide ratios for **TH1**. Association of peptides within the lipid vesicle would result in a decrease in emission intensity of NBD with an increasing mole fraction of TAMRA-labeled peptides. No energy transfer is expected in the absence of peptide association. For **TH1**, a marked decrease in F/F_0 is observed with an increasing mole fraction of acceptor peptides indicative of noncovalent association of peptides. Different association states that can be distinguished by the FRET experiments are conceivable (*32*). To model the FRET data, the following assumptions were made: the fluorescence of a donor molecule is quenched only if at least one acceptor is present in the oligomer. In addition, one acceptor has the ability to quench all donors within that oligomer. With a

random number of donors and acceptors in the aggregates, the total number of quenched donors (N_Q) and unquenched donors (N_D) follows a binominal distribution. N_Q and N_D are related to relative fluorescence F/F_0 measured in the experiment according to eq 1:

$$\frac{F}{F_0} = 1 - \left(1 - \frac{f_Q}{f_D}\right)\frac{N_Q}{N_D} \quad (1)$$

where F is the fluorescence in the presence of the acceptor, F_0 that in its absence, f_D the molar fluorescence of unquenched donor D, and f_Q that of quenched donor D. With the relationship $X_A + X_D + X_u = 1$, where the mole fraction of the acceptor peptide is given by X_A, that of the donor by X_D, and that of the unlabeled peptide by X_U, and the assumption of a monomer−oligomer equilibrium, the following expression can be written to describe a monomer−dimer equilibrium (eq 2):

$$\frac{F}{F_0} = m + (1 - m)\left(1 - X_D\frac{X_A}{X_D}\right) \quad (2)$$

where m is the fraction of the peptides in the monomeric state and $1 - m$ that of the peptides in the oligomeric state. The equation for a monomer−trimer equilibrium can be written as (eq 3)

$$\frac{F}{F_0} = m + (1 - m)\left[1 - {X_D}^2\left(\frac{2}{X_D}\right)\left(\frac{X_A}{X_D}\right) - \left(\frac{X_A}{X_D}\right)^2\right] \quad (3)$$

The dissociation constant K_D is then defined as (eq 4)

$$K_D = \frac{(mX_P)^n}{(1 - m)X_P/n} \quad (4)$$

where X_P is the lipid-to-peptide ratio and n the oligomer number (for further details, see the Supporting Information). Assuming a monomer−dimer equilibrium, a global fit analysis results in the dotted lines. The data fit best to a monomer−trimer equilibrium, where the FRET curves for **TH1** obtained at different lipid-to-peptide ratios are well described (Figure 4). A dissociation constant K_D of 4.3×10^{-6} MF^2 was obtained from global fit analysis (*33*).

Control of Peptide Association. As outlined above, **TH1** does not insert into DPPC in the crystalline state, while it inserts with reasonable efficiency into POPC, which forms a liquid-crystalline phase at room temperature. If the peptide is restricted to the liquid-crystalline phase and the association of **TH1** is concentration-dependent, we expected to control its aggregation state in lipid vesicles by temperature, thus controlling the crystalline and liquid-crystalline domains of a lipid mixture. It is known that DPPC and POPC are fully miscible in the liquid-crystalline (L_α) phase at elevated temperatures, while they phase separate into an L_α and a crystalline phase at lower temperatures. We chose a DPPC/POPC lipid mixture with a molar ratio of 6:4, which is known to be in the liquid-crystalline phase above 34 °C and is phase separated at temperatures below 34 °C (*34*). In the two-phase coexistence regime, crystalline phase DPPC-rich domains exist in an extended network structure surrounded by liquid-crystalline POPC (*35*). The expected phase transition of DPPC/POPC (6:4) large unilamellar vesicles (LUVs) from the crystalline/liquid-crystalline coexistence phase to a liquid-crystalline phase was corroborated using the fluorophore Patman (Figure 5). Patman [6-hexadecanoyl-2-({[2-(trimethylammonium)ethyl]methyl}amino)naphthalene chloride] and the structurally related fluorophore Prodan [6-propionyl-2-(dimethylamino)naphthalene] are localized in the phospholipid headgroup region and show a large Stokes shift when crossing the phase transition temperature from the gel phase to the liquid-crystalline phase (*36*, *37*). The observed red shift indicates the polarity sensitivity of the fluorescent probes (*37*, *38*). Figure 5 shows the fluorescence maximum of Patman embedded in DPPC/POPC (6:4) LUVs as a function of temperature. The fluorescence maximum increases from 429 to 466 nm with a turning point at 34 °C indicating the transition from a crystalline/liquid-crystalline coexistence phase to a liquid-crystalline phase.

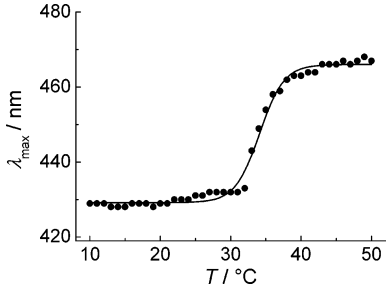

FIGURE 5: Determination of phase transition temperature T_m of a mixture of DPPC and POPC in a molar ratio of 6:4 by means of Patman fluorescence. The Patman fluorescence intensity as a function of temperature was monitored for a lipid-to-fluorophore ratio of 100:1. The solid line is the result of a Boltzmann fit, whose inflection point delivers a phase transition temperature T_m of 34 °C.

In this DPPC/POPC lipid mixture, **TH1** was inserted and its association behavior analyzed by temperature-dependent FRET measurements. Figure 6A displays the donor fluorescence intensity as a function of temperature for NBD-**TH1** inserted in unilamellar vesicles in the presence and absence of acceptor 5(6)-TAMRA-**TH1**. The donor fluorescence intensity of DPPC/POPC LUVs containing only NBD-**TH1** decays almost linearly with an increase in temperature. The observed decay in intensity can mostly be attributed to the decrease in NBD quantum yield with an increase in temperature (*39*). When both donor- and acceptor-labeled peptides are present in the vesicles, the donor fluorescence intensity is considerably decreased at lower temperatures. The low donor fluorescence intensity is caused by energy transfer to the acceptor. The fluorescence intensity of the donor shows a modest increase with temperature to 33 °C. At 33 °C, a well-defined maximum in donor fluorescence intensity is observed. Above this temperature, the fluorescence intensity of NBD decreases almost in the same manner as that of the NBD-**TH1**-doped DPPC/POPC LUVs lacking the acceptor peptide. To discern the temperature dependence of the donor fluorescence in the absence of acceptor, the ratio of donor fluorescence intensity in the presence and absence of acceptor [$I_{NBD}/I_{NBD+5(6)-TAMRA}$] was plotted (Figure 6B). The ratio exhibits a positive slope in the entire temperature range, consistent with the idea that the energy transfer efficiency decreases with an increase in temperature. However, at 35 °C a clearly discernible change in slope can be observed from 20 to 8.5 mK^{-1}. The observed maximum

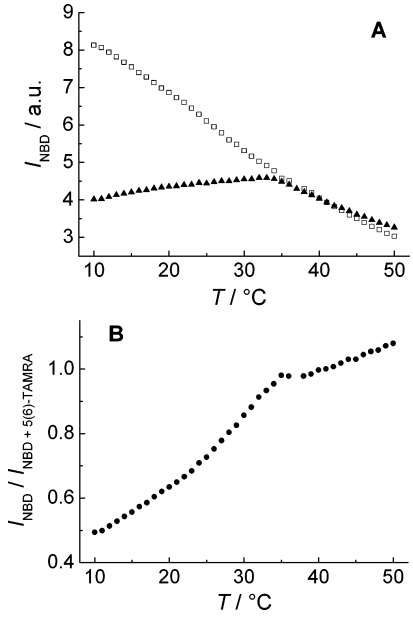

FIGURE 6: (A) Temperature dependence of the NBD-**TH1** fluorescence intensity obtained for unilamellar DPPC/POPC vesicles in a molar ratio of 6:4 in the absence (□) and presence (▲) of 5(6)-TAMRA-**TH1**. (B) Ratio of the donor fluorescence intensity in the presence of 5(6)-TAMRA-**TH1** (□ shown in panel A) and the fluorescence intensity of NBD-**TH1** in its absence (▲ shown in panel A) as a function of temperature.

in fluorescence intensity of the donor (Figure 6A) and change in slope (Figure 6B) occurs within a temperature range of 33−35 °C, consistent with the phase transition of the DPPC/POPC lipid mixture from crystalline/liquid-crystalline coexistence region to the liquid-crystalline phase with a T_m of 34 °C.

DISCUSSION

Clustering of proteins in the cell membrane in domains and subsequent oligomerization are related processes and may be necessary for their function. For instance, heterodimerization is required for the formation of a functional $GABA_B$ receptor (*40*, *41*). Proper insertion into a lipid bilayer is a necessary prerequisite for a designed transmembrane synthetic peptide ensemble. We investigated the integration of **TH1** in DPPC and POPC lipid vesicles with the conclusion that the lipid must be in the liquid-crystalline state for the peptide to partition from the aqueous to the membrane phase. We observed unexpected sigmoidally shaped curves in titrations where the lipid:peptide ratio was varied (see Figure 2). Below a lipid-to-peptide ratio of 200:1, almost no detectable peptide insertion into POPC vesicles on a time scale of 20 min is observed. An explanation for this behavior might be found in peptide oligomer (or peptide micelles) formation in the aqueous solution, which may hinder or slow the insertion process at high peptide and low lipid concentrations. Peptide oligomer formation competes with the insertion of the peptide in the lipid vesicles. Once inserted, **TH1** is capable of switching between the different vesicle populations. To ensure a reproducible lipid-to-peptide ratio and a fast equilibrium, we adopted addition of the peptide to the lipid film prior to vesicle formation for the investigation of the aggregation state of **TH1** in vesicles.

Choma et al. (*24*) and Zhou et al. (*23*) have investigated the oligomerization propensity of similar peptide sequences in detergent micelles and found that such peptides form dimers or trimers in lipid environments. Here, we investigated the association state of **TH1** in zwitterionic phospholipid vesicles. From a global fit analysis of our FRET data, we conclude that **TH1** forms trimers in lipid vesicles. A

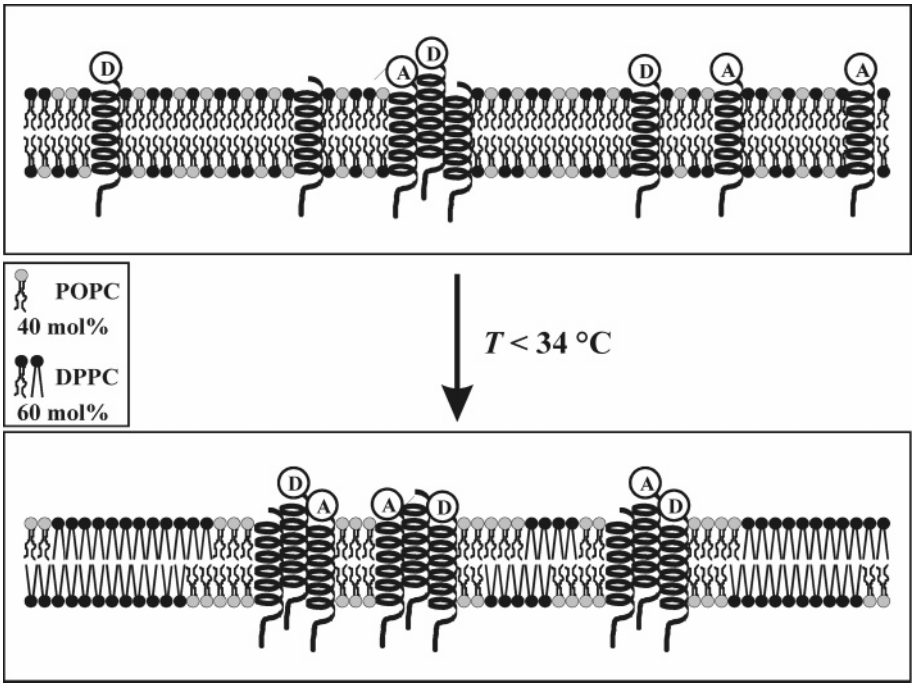

FIGURE 7: Schematic illustration of temperature-triggered domain exclusion of **TH1** and subsequent concentration-driven self-assembly. Below the phase transition temperature of 34 °C, DPPC is in the crystalline state forming long, thin membrane phase-separated domains with a network configuration within a fluid POPC matrix. Peptide **TH1** is excluded from the crystalline phase DPPC domains. Increasing the temperature above the phase transition temperature disperses the DPPC domains, and a completely miscible liquid-crystalline membrane occurs in which the peptide is fully soluble. The increase in the accessible lipid phase for the peptide leads to a larger lipid-to-peptide ratio, leading to a decrease in the level of formation of oligomers.

reversible equilibrium between monomers and trimers is established, which is indicated by the increase in the monomer fraction with an increase in lipid concentration. Previous work has firmly established that a central asparagine or other polar residues such as Gln, Asp, or Glu (*24*, *42*) are capable of promoting helix−helix interactions in membrane environments. Replacement of the polar residue abolished all association in their respective cases.

The formation of oligomers in a concentration-dependent manner and the observation that **TH1** does not partition into lipids in the crystalline state led us to hypothesize that the oligomerization state of the peptide may be controlled by the physical state of the lipid membrane. We demonstrate here the temperature-triggered domain exclusion of **TH1** and subsequent concentration-driven self-assembly. The self-assembly process described here is reminiscent of lipid rafts that result in transient microdomain formation, and have been invoked to explain the biological activity of a wide variety of membrane-embedded proteins. This remarkable oligomerization process was observed by monitoring the efficiency of fluorescence resonance energy transfer between donor and acceptor peptides. The FRET data obtained for a mixture of DPPC and POPC in a molar ratio of 6:4 display a maximum in donor fluorescence intensity (Figure 6), i.e., a minimum in energy transfer efficiency at phase transition temperature T_m. The significant change in fluorescence correlates with the phase transition temperature of this mixture. Below the phase transition temperature of 34 °C, DPPC is in the crystalline state forming long, thin membrane phase-separated domains with a network configuration within a fluid POPC matrix (*34*, *35*). Our insertion studies of **TH1** have shown that the peptide does not insert in DPPC bilayers at room temperature, which can be attributed to the fact that the lipid is in the crystalline state. From this, we suppose that below the phase transition temperature T_m of 34 °C of the POPC/DPPC lipid mixture **TH1** is excluded from the crystalline phase DPPC domains, and hence, the apparent lipid-to-peptide ratio in the POPC matrix is lower. Increasing the temperature above the phase transition temperature disperses the DPPC domains, and a completely miscible liquid-crystalline membrane in which the peptide is fully soluble occurs (Figure 7). The increase in the accessible lipid phase for the peptide leads to a larger lipid-to-peptide ratio, leading to a decrease in energy transfer efficiency.

CONCLUSION

The formation of lipid rafts and sequestration of proteins and other membrane-embedded agents have been frequently invoked in the recent past to explain biological activity. We have described the modulation of reversible association of a peptide system capable of insertion into a lipid bilayer in the liquid-crystalline state but not when it is in a crystalline state. The results described here set the stage for more sophisticated experiments in which multiple membrane components could be controlled in a rational manner simply by changing the physical state of the bilayer matrix.

ACKNOWLEDGMENT

We thank B. Dick for his help in the global fit analysis of the FRET data.

SUPPORTING INFORMATION AVAILABLE

CD spectrum of **TH1** in POPC vesicles (Figure 1S) and theoretical treatment of FRET data. This material is available free of charge via the Internet at http://pubs.acs.org.

REFERENCES

1. Stevens, T. J., and Arkin, I. T. (2000) Do more complex organisms have a greater proportion of membrane proteins in their genomes? *Proteins 39*, 417−420.
2. Curran, A. R., and Engelman, D. M. (2003) Sequence motifs, polar interactions and conformational changes in helical membrane proteins, *Curr. Opin. Struct. Biol. 13*, 412−417.
3. Lemmon, M. A., Flanagan, J. M., Treutlein, H. R., Zhang, J., and Engelman, D. M. (1992) Sequence specificity in the dimerization of transmembrane α-helices, *Biochemistry 31*, 12719−12725.
4. Lemmon, M. A., Treutlein, H. R., Adams, P. D., Brunger, A. T., and Engelman, D. M. (1994) A dimerization motif for transmembrane α-helices, *Nat. Struct. Biol. 1*, 157−163.
5. Langosch, D., Brosig, B., Kolmar, H., and Fritz, H. J. (1996) Dimerisation of the glycophorin A transmembrane segment in membranes probed with the ToxR transcription activator, *J. Mol. Biol. 263*, 525−530.
6. Deber, C. M., Khan, A. R., Li, Z. M., Joensson, C., Glibowicka, M., and Wang, J. (1993) Val-Ala mutations selectively alter helix-helix packing in the transmembrane segment of phage M13 coat protein, *Proc. Natl. Acad. Sci. U.S.A. 90*, 11648−11652.
7. Arkin, I. T., Adams, P. D., Mackenzie, K. R., Lemmon, M. A., Brunger, A. T., and Engelman, D. M. (1994) Structural organization of the pentameric transmembrane α-helices of phospholamban, a cardiac ion-channel, *EMBO J. 13*, 4757−4764.
8. Simmerman, H. K. B., Kobayashi, Y. M., Autry, J. M., and Jones, L. R. (1996) A leucine zipper stabilizes the pentameric membrane domain of phospholamban and forms a coiled-coil pore structure, *J. Biol. Chem. 271*, 5941−5946.
9. Manolios, N., Bonifacino, J. S., and Klausner, R. D. (1990) Transmembrane helical interactions and the assembly of the T-cell receptor complex, *Science 249*, 274−277.
10. Cosson, P., and Bonifacino, J. S. (1992) Role of transmembrane domain interactions in the assembly of class-II MHC molecules, *Science 258*, 659−662.
11. Popot, J. L., and Engelman, D. M. (2000) Helical membrane protein folding, stability, and evolution, *Annu. Rev. Biochem. 69*, 881−922.
12. Engelman, D. M., Chen, Y., Chin, C. N., Curran, A. R., Dixon, A. M., Dupuy, A. D., Lee, A. S., Lehnert, U., Matthews, E. E., Reshetnyak, Y. K., Senes, A., and Popot, J. L. (2003) Membrane protein folding: Beyond the two stage model, *FEBS Lett. 555*, 122−125.
13. Bilgiçer, B., and Kumar, K. (2004) De novo design of defined helical bundles in membrane environments, *Proc. Natl. Acad. Sci. U.S.A. 101*, 15324−15329.
14. Langosch, D., and Heringa, J. (1998) Interaction of transmembrane helices by a knobs-into-holes packing characteristic of soluble coiled coils, *Proteins 31*, 150−159.
15. Lupas, A. (1996) Coiled coils: New structures and new functions, *Trends Biochem. Sci. 21*, 375−382.
16. Bilgiçer, B., and Kumar, K. (2003) Protein design using unnatural amino acids, *J. Chem. Educ. 80*, 1275−1281.
17. Yoder, N. C., and Kumar, K. (2002) Fluorinated amino acids in protein design and engineering, *Chem. Soc. Rev. 31*, 335−341.
18. Bilgiçer, B., Xing, X., and Kumar, K. (2001) Programmed self-sorting of coiled coils with leucine and hexafluoroleucine cores, *J. Am. Chem. Soc. 123*, 11815−11816.
19. Bilgiçer, B., Fichera, A., and Kumar, K. (2001) A coiled coil with a fluorous core, *J. Am. Chem. Soc. 123*, 4393−4399.
20. Bilgiçer, B., and Kumar, K. (2002) Synthesis and thermodynamic characterization of self-sorting coiled coils, *Tetrahedron 58*, 4105−4112.
21. Li, H. M., Cocco, M. J., Steitz, T. A., and Engelman, D. M. (2001) Conversion of phospholamban into a soluble pentameric helical bundle, *Biochemistry 40*, 6636−6645.
22. Slovic, A. M., Summa, C. M., Lear, J. D., and DeGrado, W. F. (2003) Computational design of a water-soluble analog of phospholamban, *Protein Sci. 12*, 337−348.

23. Zhou, F. X., Cocco, M. J., Russ, W. P., Brunger, A. T., and Engelman, D. M. (2000) Interhelical hydrogen bonding drives strong interactions in membrane proteins, *Nat. Struct. Biol. 7*, 154−160.
24. Choma, C., Gratkowski, H., Lear, J. D., and DeGrado, W. F. (2000) Asparagine-mediated self-association of a model transmembrane helix, *Nat. Struct. Biol. 7*, 161−166.
25. Gratkowski, H., Lear, J. D., and DeGrado, W. F. (2001) Polar side chains drive the association of model transmembrane peptides, *Proc. Natl. Acad. Sci. U.S.A. 98*, 880−885.
26. Simons, K., and Vaz, W. L. C. (2004) Model systems, lipid rafts, and cell membranes, *Annu. Rev. Biophys. Biomol. Struct. 33*, 269−295.
27. Wimley, W. C., and White, S. H. (2000) Designing transmembrane α-helices that insert spontaneously, *Biochemistry 39*, 4432−4442.
28. Chung, L. A., Lear, J. D., and DeGrado, W. F. (1992) Fluorescence studies of the secondary structure and orientation of a model ion channel peptide in phospholipid vesicles, *Biochemistry 31*, 6608−6616.
29. Reddy, L. G., Jones, L. R., and Thomas, D. D. (1999) Depolymerization of phospholamban in the presence of calcium pump: A fluorescence energy transfer study, *Biochemistry 38*, 3954−3962.
30. London, E., and Khorana, H. G. (1982) Denaturation and renaturation of bacteriorhodopsin in detergents and lipid-detergent mixtures, *J. Biol. Chem. 257*, 7003−7011.
31. Li, M., Reddy, L. G., Bennett, R., Silva, N. D., Jr., Jones, L. R., and Thomas, D. D. (1999) A fluorescence energy transfer method for analyzing protein oligomeric structure: Application to phospholamban, *Biophys. J. 76*, 2587−2599.
32. Adair, B. D., and Engelman, D. M. (1994) Glycophorin A helical transmembrane domains dimerize in phospholipid bilayers: A resonance energy transfer study, *Biochemistry 33*, 5539−5544.
33. Expressed in units of peptide/lipid mole fraction (MF).
34. Curatolo, W., Sears, B., and Neuringer, L. J. (1985) A calorimetry and deuterium NMR study of mixed model membranes of 1-palmitoyl-2-oleoylphosphatidylcholine and saturated phosphatidylcholines, *Biochim. Biophys. Acta 817*, 261−270.
35. Shoemaker, S. D., and Vanderlick, T. K. (2003) Material studies of lipid vesicles in the L_α and L_α-gel coexistence regimes, *Biophys. J. 84*, 998−1009.
36. Massey, J. B., She, H. S., and Pownall, H. J. (1985) Interfacial properties of model membranes and plasma lipoproteins containing ether lipids, *Biochemistry 24*, 6973−6978.
37. Hutterer, R., Schneider, F. W., Sprinz, H., and Hof, M. (1996) Binding and relaxation behaviour of prodan and patman in phospholipid vesicles: A fluorescence and ^{1}H NMR study, *Biophys. Chem. 61*, 151−160.
38. Lippert, E. (1957) Spektroskopische Bestimmung des Dipolmomentes aromatischer Verbindungen im ersten angeregten Singulettzustand, *Z. Elektrochem. 61*, 962−975.
39. Fery-Forgues, S., Fayet, J., and Lopez, A. (1993) Drastic changes in the fluorescence properties of NBD probes with the polarity of the medium: Involvement of TICT state? *J. Photochem. Photobiol., A 70*, 229−243.
40. White, J. H., Wise, A., Main, M. J., Green, A., Fraser, N. J., Disney, G. H., Barnes, A. A., Emson, P., Foord, S. M., and Marshall, F. H. (1998) Heterodimerization is required for the formation of a functional $GABA_B$ receptor, *Nature 396*, 679−682.
41. Kammerer, R. A., Frank, S., Schulthess, T., Landwehr, R., Lustig, A., and Engel, J. (1999) Heterodimerization of a functional $GABA_B$ receptor is mediated by parallel coiled-coil α-helices, *Biochemistry 38*, 13263−13269.
42. Lear, J. D., Gratkowski, H., and DeGrado, W. F. (2001) De novo design, synthesis and characterization of membrane-active peptides, *Biochem. Soc. Trans. 29*, 559−564.

BI050096F